NEUROSURGICAL FOCUS

Neurosurg Focus 56(4):E2, 2024

360° around the orbit: key surgical anatomy of the microsurgical and endoscopic cranio-orbital and orbitocranial approaches

Edoardo Agosti, MD,[1–3] A. Yohan Alexander, BA,[1,2,4] Pedro Plou, MD,[1,2,5] Luciano C. P. C. Leonel, PhD,[1,2] Alessandro De Bonis, MD,[1,2,6] Megan M. J. Bauman, MS,[1,2] Ainhoa García-Lliberós, MD, PhD,[1,2,7] Amedeo Piazza, MD,[1,2,8] Fabio Torregrossa, MD,[1,2,9] Carlos D. Pinheiro Neto, MD, PhD,[1,2,10] and Maria Peris Celda, MD, PhD[1,2,10]

[1]Rhoton Neurosurgery and Otolaryngology Surgical Anatomy Program, Mayo Clinic, Rochester, Minnesota; [2]Department of Neurologic Surgery, Mayo Clinic, Rochester, Minnesota; [3]Division of Neurosurgery, Department of Medical and Surgical Specialties, Radiological Sciences and Public Health, University of Brescia, Italy; [4]Medical School, University of Minnesota, Minneapolis, Minnesota; [5]Department of Neurosurgery, Hospital Italiano de Buenos Aires, Argentina; [6]Department of Neurosurgery and Gamma Knife Radiosurgery, I.R.C.C.S. San Raffaele Scientific Institute, Vita-Salute University, Milan, Italy; [7]Department of Otolaryngology, Valencia University General Hospital, Valencia, Spain; [8]Department of Neuroscience, "Sapienza" University, Rome, Italy; [9]Neurosurgical Unit, Department of Biomedicine, Neurosciences and Advanced Diagnostics (BiND), University of Palermo, Italy; and [10]Department of Otolaryngology/Head and Neck Surgery, Mayo Clinic, Rochester, Minnesota

OBJECTIVE Several pathologies either invade or arise within the orbit. These include meningiomas, schwannomas, and cavernous hemangiomas among others. Although several studies describing various approaches to the orbit are available, no study describes all cranio-orbital and orbitocranial approaches with clear, surgically oriented anatomical descriptions. As such, this study aimed to provide a comprehensive guide to the microsurgical and endoscopic approaches to and through the orbit.

METHODS Six formalin-fixed, latex-injected cadaveric head specimens were dissected in the surgical anatomy laboratory at the authors' institution. In each specimen, the following approaches were modularly performed: endoscopic transorbital approaches (ETOAs), including a lateral transorbital approach and a superior eyelid crease approach; endoscopic endonasal approaches (EEAs), including those to the medial orbit and optic canal; and transcranial approaches, including a supraorbital approach, a fronto-orbital approach, and a 3-piece orbito-zygomatic approach. Each pertinent step was 3D photograph–documented with macroscopic and endoscopic techniques as previously described.

RESULTS Endoscopic endonasal approaches to the orbit afforded excellent access to the medial orbit and medial optic canal. Regarding ETOAs, the lateral transorbital approach afforded excellent access to the floor of the middle fossa and, once the lateral orbital rim was removed, the cavernous sinus could be dissected and the petrous apex drilled. The superior eyelid approach provides excellent access to the anterior cranial fossa just superior to the orbit, as well as the dura of the lesser wing of the sphenoid. Craniotomy-based approaches provided excellent access to the anterior and middle cranial fossa and the cavernous sinus, except the supraorbital approach had limited access to the middle fossa.

CONCLUSIONS This study outlines the essential surgical steps for major cranio-orbital and orbitocranial approaches. Endoscopic endonasal approaches offer direct medial access, potentially providing bilateral exposure to optic canals. ETOAs serve as both orbital access and as a corridor to surrounding regions. Cranio-orbital approaches follow a lateral-to-medial, superior-to-inferior trajectory, progressively allowing removal of protective bony structures for proportional orbit access.

https://thejns.org/doi/abs/10.3171/2024.1.FOCUS23866

KEYWORDS orbit; approaches; cranio-orbital; orbitocranial; endoscopic transorbital; skull base

ABBREVIATIONS CN = cranial nerve; EEA = endoscopic endonasal approach; ETOA = endoscopic transorbital approach; ICA = internal carotid artery; IOA = infraorbital artery; IOF = inferior orbital fissure; ION = infraorbital nerve; MOB = meningo-orbital band; OA = ophthalmic artery; OC = optic canal; ON = optic nerve; SOF = superior orbital fissure.

SUBMITTED December 1, 2023. **ACCEPTED** January 30, 2024.
INCLUDE WHEN CITING DOI: 10.3171/2024.1.FOCUS23866.

The orbit is a conical space that sits just inferior to the anterior cranial fossa, anterior to the middle cranial fossa, superior to the maxillary sinus, and medial to the nasal cavity. It houses several neurovascular structures that are vital for vision and extraocular motility. Given its close relationship to many anatomical areas of the skull base, several pathologies either invade or arise within the orbit.[1–4]

To resect lesions in and around the orbit, several approaches have been described, including craniotomies with modular removal of the superior and lateral walls of the orbit, endoscopic endonasal approaches (EEAs), and more recently, microscopic and endoscopic transorbital approaches (ETOAs).[2–10] Given the many intricate approaches to the orbit, their appropriate selection and successful execution requires an in-depth knowledge of their key steps and anatomical indications and limitations.[11–17]

Although several studies describing various approaches to the orbit are available, no study describes all cranio-orbital and orbitocranial approaches with clear, surgically oriented anatomical descriptions. As such, this study aims to provide a comprehensive guide to the microsurgical and endoscopic approaches to and through the orbit.

Methods

All aspects of this study were approved by our Institutional Review Board and Biospecimens Committee, as required by standard protocols.

Six cadaveric specimens were dissected in the surgical anatomy laboratory at our institution. All specimens were formalin-fixed and latex-injected using the 6-vessel technique.[18] We used 0°, 30°, and 45° endoscopes (4-mm outer diameter, 18-cm working length, Hopkins II, Karl Storz) attached to a high-definition camera and a digital video recorder system, as well as an operating microscope (Leica Microsystems M844 F40) together with a complete set of instruments, for endoscopic and microsurgical skull base surgery.

The following approaches were modularly performed in each specimen: ETOAs, including a lateral transorbital approach and a superior eyelid crease approach; EEAs, including those to the medial orbit and optic canal (OC); and transcranial approaches, including a supraorbital approach, a fronto-orbital approach, and a 3-piece orbitozygomatic approach.

Dissections were performed until the expected quality level was achieved and each pertinent step was 3D photograph–documented with macroscopic and endoscopic techniques, as previously described.[18]

Results

Overview of the Anatomy of the Orbit

The anatomy of the orbit is summarized in Fig. 1 and Video 1.

VIDEO 1. Photogrammetry of the orbit. © Edoardo Agosti, published with permission. Click here to view.

Endoscopic Transorbital Approaches

Patient Positioning

The specimens were in a simulated supine reverse Trendelenburg position of approximately 15°.

Lateral Transorbital Approach

A conjunctival incision was performed immediately posterior to the insertion of the lateral canthus. With a 0° endoscope, subperiosteal dissection proceeded along the lateral orbital wall. The inferior and superior limits of our exposure were the inferior orbital fissure (IOF) and the superior orbital fissure (SOF), respectively. The sutures between the greater sphenoid wing, frontal bone, and zygomatic bone were exposed and used as landmarks. Placement of a malleable retractor separated the orbital contents from the lateral wall of the orbit, creating room for further dissection. The meningo-orbital band (MOB), located at the superolateral margin of the SOF, was identified and divided—affording further medial retraction of the orbit. By progressively drilling the greater wing of the sphenoid located inferior to the SOF, superomedial to the IOF, and posterior to the zygomatic bone, a window into the temporal and middle cranial fossa was created. These corridors were divided by the sphenoid crest. The dura mater of the middle cranial fossa was progressively detached, with detachment proceeding along the middle cranial fossa. To afford more surgical freedom, the lateral orbital rim was then removed. Consequently, the ophthalmic nerve and maxillary nerve were identified. The middle meningeal artery was divided, exposing the foramen ovale and mandibular nerve. The cavernous sinus and Meckel's cave were fully dissected, affording access to cranial nerve (CN) III, CN IV, CN V1–3, and CN VI. The petrous apex was then drilled and the posterior fossa dura was opened, which provided access to the ventrolateral brainstem. The pertinent steps and relevant surgical anatomy of the lateral transorbital approach can be seen in Figs. 2 and 3.

Superior Eyelid Approach

A skin incision was performed at level of the supratarsal fold. The superior tarsus and levator palpebrae superioris muscle were identified and the superior orbital rim was detached from the periorbita. With the aid of a 0° endoscope, subperiosteal dissection was continued posteriorly along the orbital roof. The anterior and posterior ethmoidal foramina were identified in the medial aspect of the surgical corridor. A malleable retractor separated the orbital contents from the roof of the orbit, creating room for further dissection. The OC and the superior orbital fissure were identified in the posterior portion of the orbit, and a diamond burr can be used to perform the craniectomy of the anterior cranial fossa, which can be tailored to the lesion. The dura of the superior portion of the greater wing of the sphenoid bone and the anterior cranial fossa can be exposed and incised to afford adequate access to the lesion. The relevant surgical anatomy and basic anatomy of the superior eyelid approach can be seen in Fig. 4.

Preseptal Lower Eyelid Approach

The subciliary (or subtarsal) incision was made 3 to 5

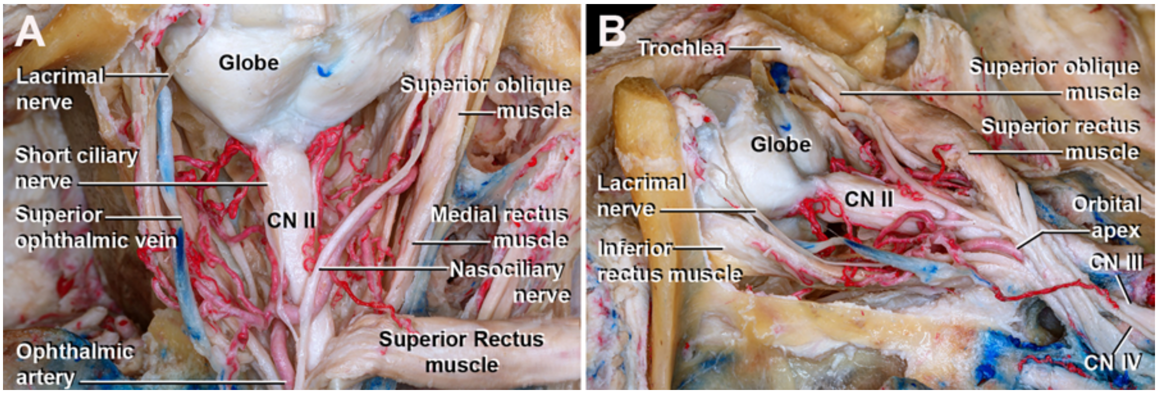

FIG. 1. A: The orbit is a cone-shaped structure housing important neurovascular structures and is protected by the orbital fat and extraocular muscles. The anatomical dissection shows the superior aspect of the orbit where the roof of the orbit and the orbital fat have been removed, exposing its anatomical features. Resection and reflection of the superior rectus muscle shows that the ON is surrounded and protected by the extraocular muscles. They are also responsible for creating the pyramidal shape and represent the most superficial landmarks when observing the orbital content after fat removal. The ophthalmic artery enters the orbital cavity via the orbital apex and, within the orbit, offers blood supply to the orbital structures from which several muscular branches branch off. **B:** With drilling of the lateral bony wall of the orbit and removal of both the periorbita and orbital fat, the lateral content of the orbit comes into view. The first structure identified is the lateral rectus muscle (representing the lateral wall of the cavity), which has been dissected and removed from this picture. The orbital apex is the region where various neurovascular structures pierce the orbital fat and enter the orbital cavity itself, among them CN III, IV, and IV, as well as V1. The inferior rectus muscle is also observed in a lateral overview representing the "floor" of the orbital content. © Edoardo Agosti, published with permission.

mm below the lower eyelid. The orbicularis oculi muscle was identified and dissection was carried out on its posterior face, which is anterior to the inferior orbital septum. This muscle was followed until reaching the inferior orbital rim, where the periosteum was incised and lifted off the orbital floor. With a 0° endoscope, subperiosteal detachment proceeds until identification of the infraorbital nerve (ION) and infraorbital artery (IOA) on the anterior surface of the inferior orbital rim. A malleable retractor was then placed to separate the orbital contents superiorly from the floor of the orbit, creating space for further dissection. Subperiosteal detachment of the orbital floor was performed along the infraorbital canal, with the zygomatic nerve serving as the lateral limit of extension for the surgical corridor, and the medial limit represented by the angle between the orbital floor and the lamina papyracea. With a diamond burr, a window was opened in the orbit floor both medially and laterally to the ION and IOA, exposing the maxillary sinus mucosa. The mucosa of the maxillary sinus was removed, providing access to the maxillary sinus (Fig. 4).

Endoscopic Endonasal Approaches

Patient Positioning and Nasal Cavity Inspection

The specimens were in a simulated supine reverse Trendelenburg position of approximately 15°.

EEA to the Medial Orbit and OC

A meticulous endoscopic examination of the nasal cavities was conducted. Subsequently, gentle medialization of the middle turbinate was performed to expose the structures within the middle meatus. With a Cottle dissector, an incision was made along the anterior border of the uncinate process, allowing entry into the ethmoid infundibulum. The uncinate process was medialized, and its superior and inferior attachments were transected using endoscopic scissors. Removal of the uncinate process facilitated clear visualization of the natural ostium of the maxillary sinus and the ethmoidal bulla. A bullectomy was then carried out, followed by resection of the ethmoid bulla with preservation of the vertical and horizontal attachments of the middle turbinate. Thru-cut forceps were employed to access the natural ostium of the maxillary sinus, and the posterior fontanelle of the maxillary sinus was excised.

The posterior ethmoid cells and superior turbinate were meticulously removed to ensure a flush border with the anterior skull base superiorly and the lamina papyracea laterally. The ostium of the sphenoid sinus was identified and enlarged superiorly toward the skull base, laterally toward the orbit, and inferiorly toward the sphenoid floor. Consequently, the medial border of the bony orbit was exposed from the OC posteriorly to the nasolacrimal duct anteriorly.

With a 45° endoscope and angled instruments, the medial wall of the orbit (lamina papyracea) was gently fractured and dissected from the periorbita and removed, and care was taken to maintain a safe distance below the ethmoid foramina to avoid damage to the ethmoidal arteries. The periorbita of the medial orbit was incised, affording access into the medial orbit. The inferior corridor to the intraconal space was identified between the medial rectus and inferior rectus muscles. Removal of orbital fat allowed visualization of the optic nerve (ON) and inferior ophthalmic vein through the medial endoscopic corridor leading to the orbit. The medial rectus muscle was retracted superiorly to enhance intraconal exposure, and the ON and ophthalmic artery (OA) could be visualized as well as the central retinal artery. The superior corridor to the intraconal space is between the superior oblique muscle and medial rectus muscle.

EEA to the OC

The bone over the OC was removed from the level of

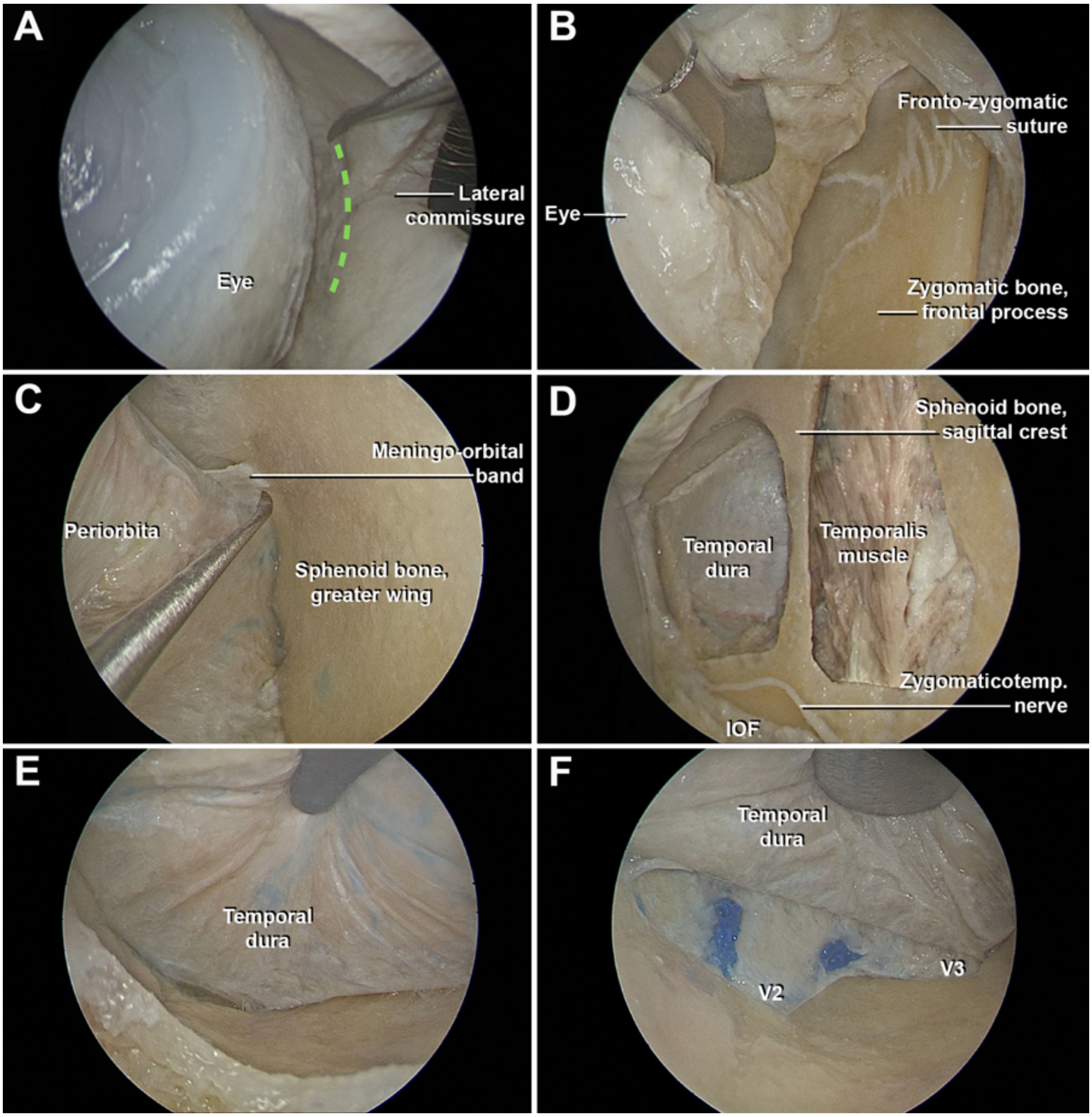

FIG. 2. The left-side endoscopic lateral transorbital approach. **A:** Incision (*dotted line*) at the lateral canthus of the left eye. **B:** Subperiosteal exposure of the lateral orbital rim, which exposes the frontozygomatic suture. **C:** Disconnection of the MOB, which then provides visualization of the SOF marking the superior boundary of bony removal. **D:** A window into the temporal fossa can be created laterally, and a window into the middle cranial fossa can be created medially. These two corridors are separated by the sphenoidal crest. **E:** Peeling the middle fossa dura off the floor of the middle fossa. **F:** Identification of V3 entering foramen ovale and V2 entering foramen rotundum. Zygomaticotemp. = zygomaticotemporal. © Edoardo Agosti, published with permission.

the prechiasmatic sulcus to the orbital apex. A horizontal incision was made in the dura mater of the OC along its superior margin, directed from proximal to distal. The anterior boundary of the incision was defined by the annulus of Zinn. Subsequently, the dural incision was extended proximally, revealing the intracranial OA and intracranial ON. The rectangular dural flap was mobilized inferiorly and completely removed, exposing the origin of the OA, intracranial OA, intracranial ON, intracanalicular OA, and intracanalicular ON. The proximal portion of the ophthalmic segment of the internal carotid artery (ICA) was also identified. The relevant surgical anatomy of the EEAs to the orbit can be found in Fig. 5.

Cranio-Orbital Approaches

Patient Positioning

The specimens were in a simulated supine position, and the head was rotated contralaterally approximately 30°.

Supraorbital Approach

The incision on the skin followed the lateral aspect of the eyebrow, with care taken to ensure that it did not to go beyond the lateral aspect of the supraorbital notch in order to protect the supraorbital nerve. Following the skin incision, subcutaneous dissection proceeded in the frontal

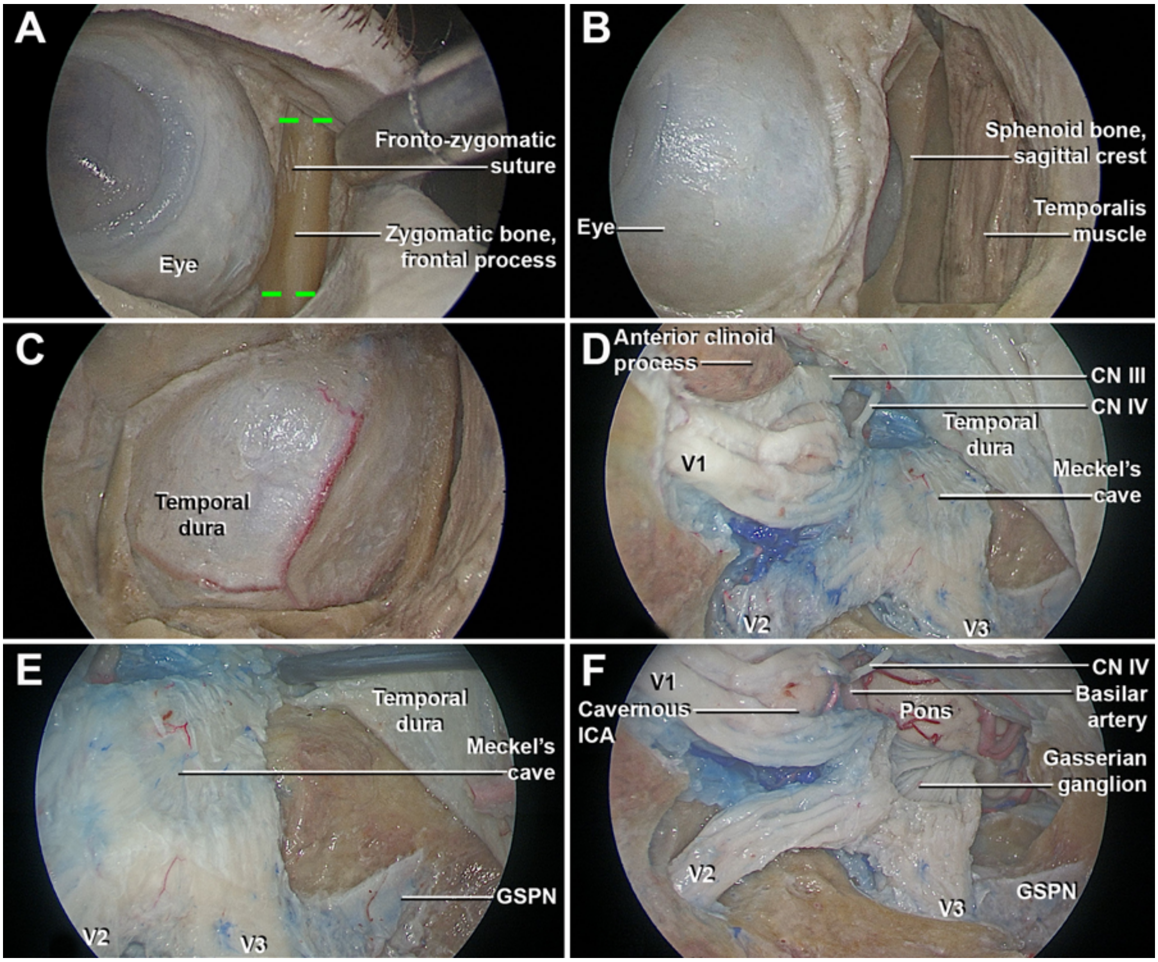

FIG. 3. Left-side endoscopic lateral transorbital approach with removal of the lateral orbital rim. **A:** Removal of the lateral orbital rim. This affords better maneuverability and thus easier dissection of the middle fossa, cavernous sinus, and petrous apex region. The *green dotted lines* represent the limit of the orbitotomy. **B:** Exposure of the temporalis muscle and temporal fossa after lateral orbitotomy. **C:** Exposure of the dura of the temporal pole temporal fossa after the lateral orbitotomy. **D:** Dissection of the cavernous sinus through the lateral orbitotomy. From superior to inferior, we can identify CN III to V3 and the cavernous portion of the ICA. **E:** Exposure of the petrous apex after cutting the middle meningeal artery. **F:** Exposure after drilling of the petrous apex and release of CN V. The lateral transorbital approach affords access to the cavernous sinus, ventrolateral brainstem, and superomedial posterior fossa. GSPN = greater superficial petrosal nerve. © Edoardo Agosti, published with permission.

direction to achieve optimal exposure of the supraorbital area. The frontal muscle was then incised parallel to the orbital rim in a medial-to-lateral direction, terminating at the superficial temporal line. A fishhook was used to retract the temporalis muscle posteriorly. A single burr hole was made at MacCarty's keyhole, approximately 8 mm superior and 5 mm posterior to the frontozygomatic suture.[12,17] Accurate placement of this burr hole exposed both the frontal dura and periorbita. After elevation of the dura away from the inner table of the frontal calvaria, a teardrop-shaped craniotomy was performed with a footplate, with its long axis parallel to the floor of the anterior cranial fossa.

Fronto-Orbital Approach

As an extension of the supraorbital approach, fronto-orbital craniotomy was extended to include the orbital roof. To remove the superior portion of the supraorbital rim, osteotomy was performed at the level of the keyhole and just medial to the supraorbital notch, and the superior orbital rim was removed after connecting the two osteotomies. The roof of the orbit and the lesser wing were then drilled. The dura was then opened in a C-shaped fashion and retracted inferiorly.

Dissection proceeded posteriorly along the roof of the orbit until the intradural anterior clinoid process and anterior petroclinoid fold were exposed. CN III, the ONs, the optic chiasm, and the ophthalmic and communicating segments of the ICA were progressively exposed. The key surgical anatomy and steps of the supraorbital and fronto-orbital craniotomy can be seen in Fig. 6.

Orbito-Zygomatic Approach

The skin incision began at the inferior border of the zygomatic arch, around 1 cm anterior to the tragus, arching upward and anteriorly and extending just behind the

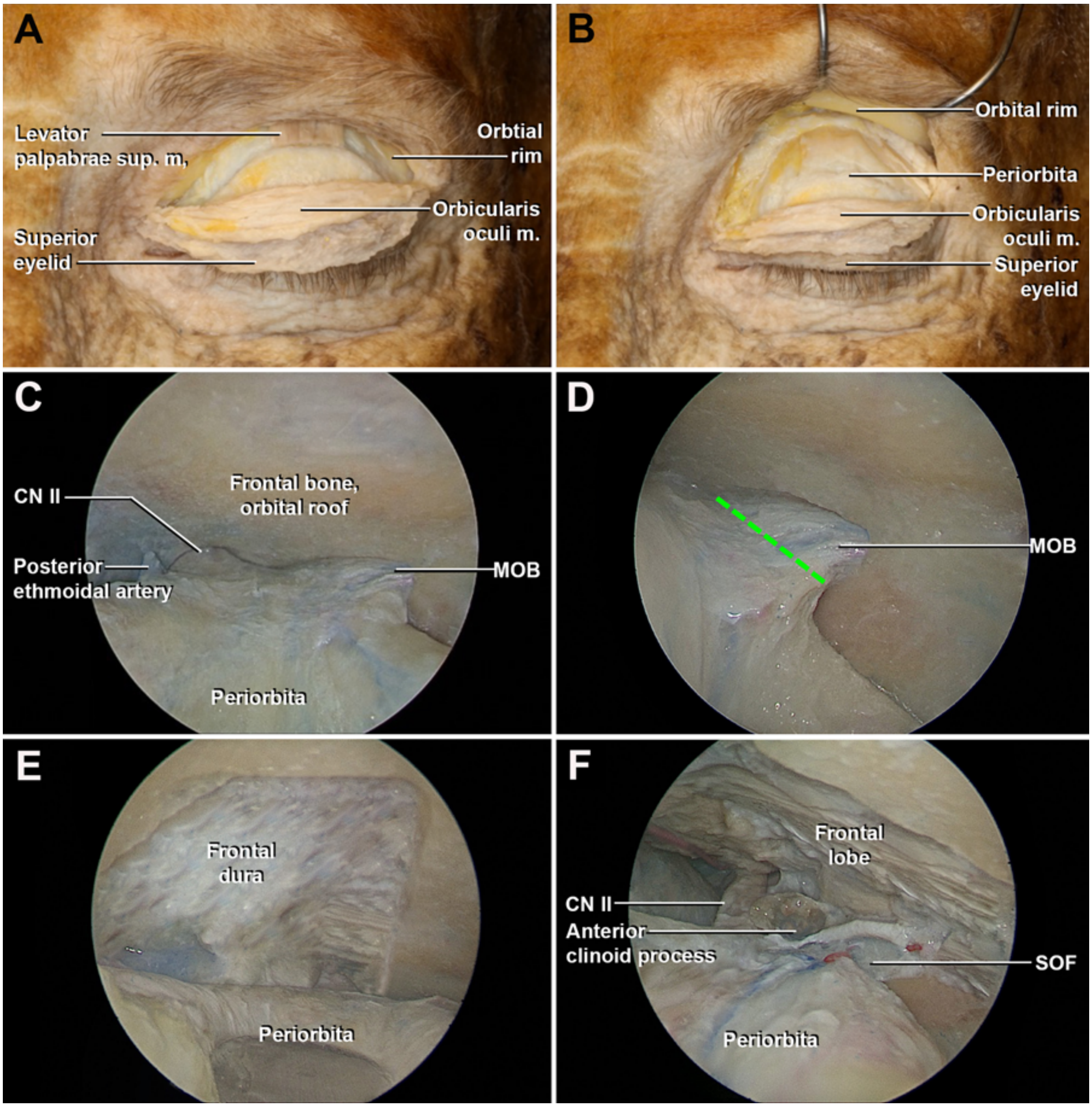

FIG. 4. Left superior eyelid approach. **A:** The superior eyelid crease approach exposing the orbicularis oculi muscle. **B:** Subperiosteal exposure of the superior orbital rim. **C:** Traveling posteriorly between the roof of the orbit superiorly and the periorbita inferiorly, we can identify the posterior ethmoidal foramen and periorbita covering its associated bundle, the OC and the periorbita covering its contents, and the SOF and its periorbita. **D:** An osteotomy is then made in the anterior cranial fossa/roof of the orbit, exposing the dura of the anterior cranial fossa. The lateral extent of the osteotomy is the lateral margin of the SOF, and the medial extent is the posterior ethmoidal foramen. The *green dotted line* represents the cut at the level of the meningo-orbital fold. **E:** The MOB is then cut to afford further inferior retraction of the orbit. **F:** The dura of the anterior cranial fossa can then be opened, providing access to the inferior frontal lobe. m. = muscle; sup. = superioris. © Edoardo Agosti, published with permission.

hairline at the contralateral midpupillary line to allow for ample retraction of the skin flap anteromedially and thus provide better orbital exposure. The dissection of the soft tissue proceeded in a subperiosteal fashion, respecting the superficial temporalis fascia. Around 2 cm behind the orbital rim, we proceeded with interfascial dissection to preserve the frontal branch of the CN VII. The temporalis muscle was progressively elevated in a subperiosteal fashion to preserve the deep temporal fascia that provides vascularization to the temporalis muscle, thereby leaving a small cuff superiorly to suture at the end of the operation.

A 3-piece orbito-zygomatic craniotomy was performed by placing the first burr hole at MacCarty's keyhole. With enlargement of this burr hole, exposure of the periorbita and frontal dura was achieved. Three other burr holes were placed, and a standard pterional craniotomy was performed. Subsequently, cuts were performed to complete the orbital optic osteotomy. The orbital cuts involved osteotomies from the MacCarty burr hole across the roof and the orbital rim medially, and from the burr hole through the lateral orbital wall and across the orbital rim laterally (Fig. 7). The orbital piece was then freed from the peri-

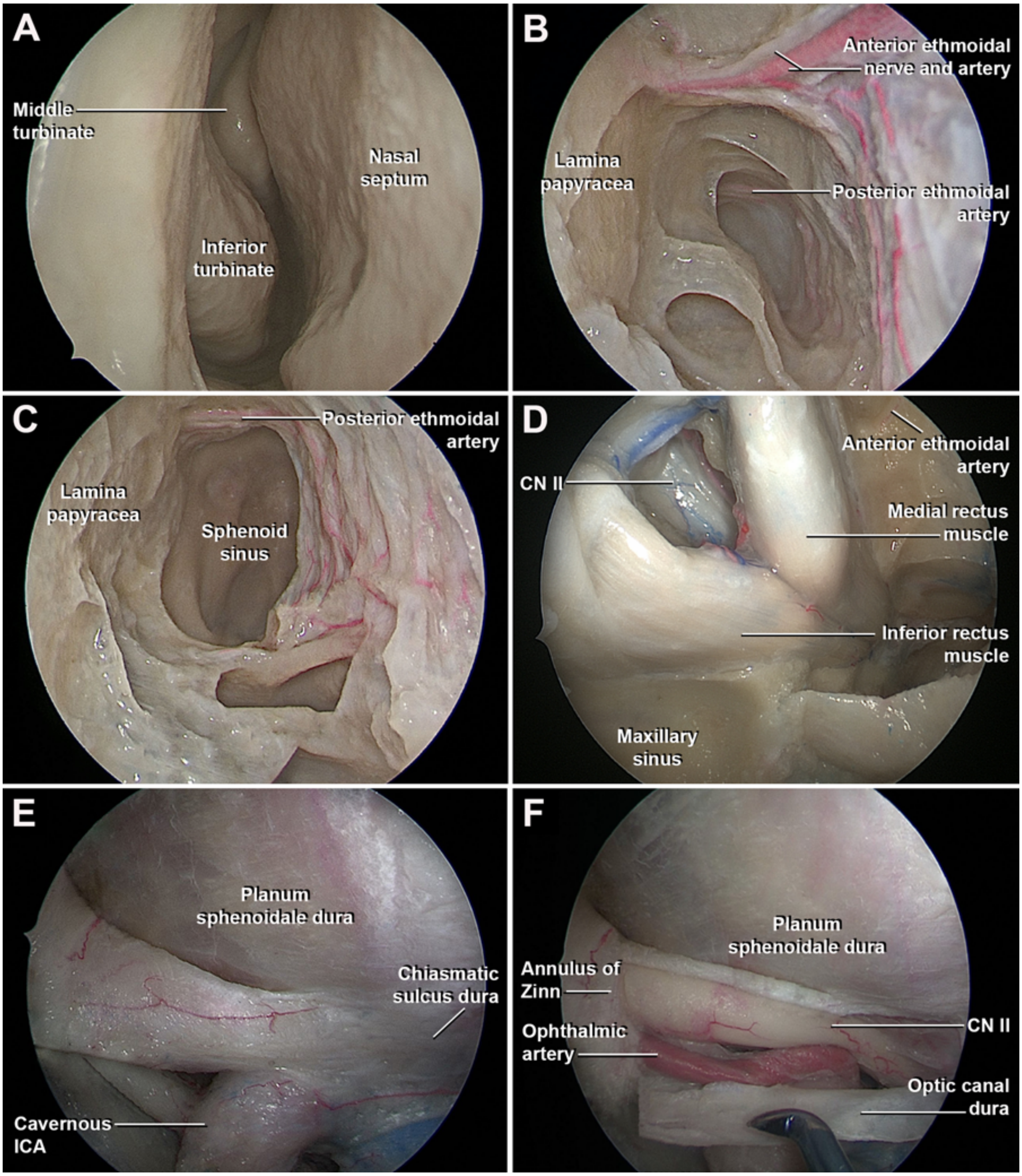

FIG. 5. Right-sided endoscopic endonasal approach to the medial orbit and OC. **A:** Overview of the right nasal cavity depicting the middle and superior turbinates. **B:** Progressive removal of structures within the middle meatus with preservation of the middle turbinate laterally. Preservation of the middle turbinate is possible when approaching the medial orbit and OC but is not necessary. **C:** Exposure of the lamina papyracea laterally and the posterior wall of the sphenoid sinus posteriorly. **D:** After removal of the periorbita and dissection through the periorbital fat, the inferomedial corridor through the orbit is seen between the medial and inferior rectus muscles. **E:** View of the dura overlying the optic canal at the level of the posterior wall of the sphenoid sinus. **F:** After the dura of the OC is opened, the ON and OA are seen in their intracranial and intracanalicular segments. © Edoardo Agosti, published with permission.

orbita and removed. Zygomatic osteotomy was performed with a bony cut at the anterior aspect of the zygomatic arch and an oblique cut at the posterior aspect of the zygomatic arch, with care taken not to enter the temporomandibular joint capsule. The masseter was left attached to the freed zygomatic arch, and the bone and muscle were reflected inferiorly.

After craniotomy was completed in an extradural fashion, the lesser wing was progressively drilled to the MOB. The MOB was divided, and the SOF and cavernous sinus

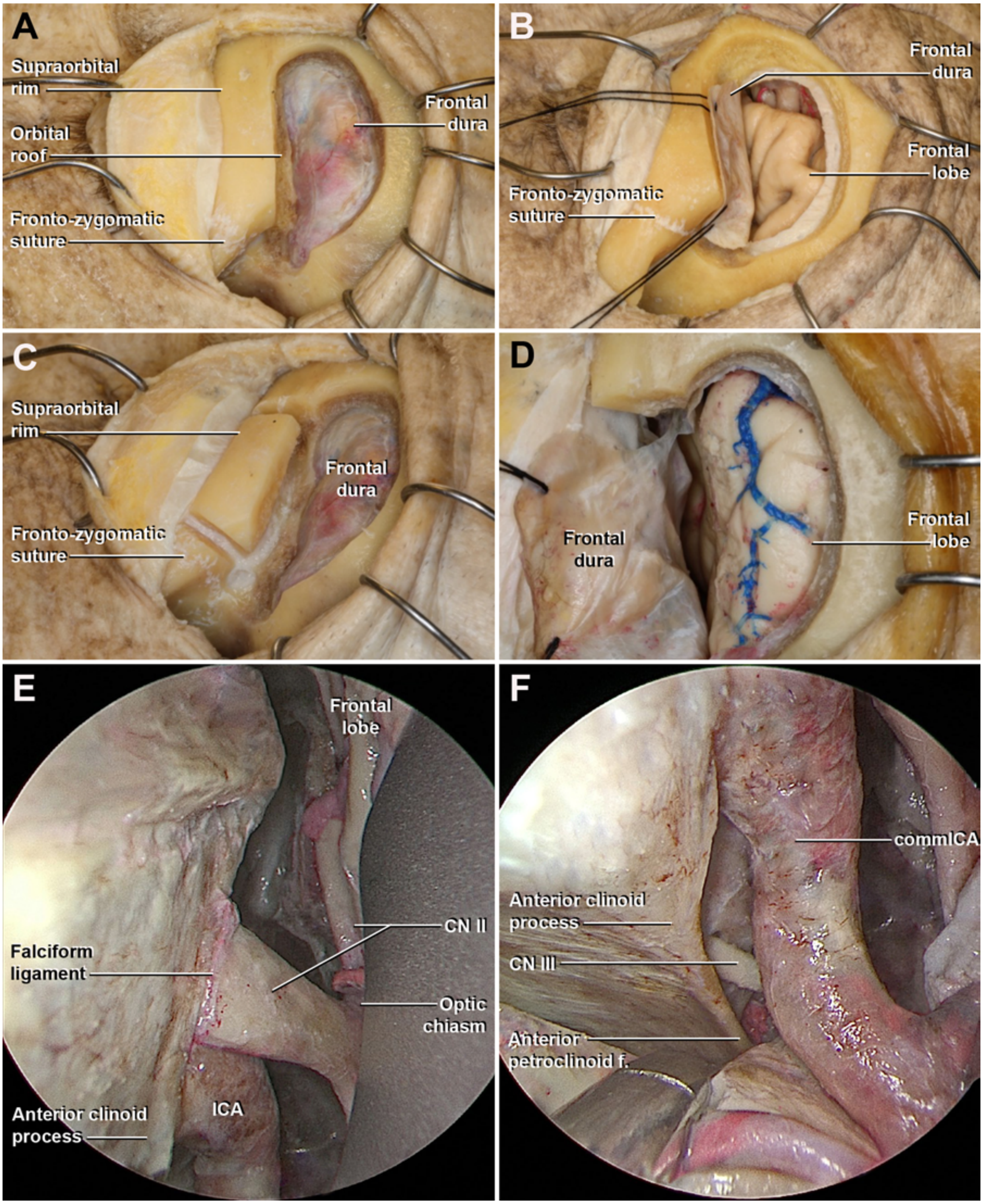

FIG. 6. Left-side supraorbital approach and associated osteotomy of the superior orbit. **A:** View of the supraorbital craniotomy after an eyebrow skin incision. **B:** C-shaped durotomy after supraorbital craniotomy affording access to the anterior cranial fossa and anterior portion of the frontal inferior frontal gyrus. **C:** Osteotomy of the orbital roof. **D:** Inferior dural reflection after the superior orbital rim has been removed and the roof of the orbit has been drilled away. **E:** View of the optico-carotid and interoptic triangles after supraorbital craniotomy with a 0° endoscope. **F:** Identification of the CN III in the oculomotor cistern. commICA = communicating segment of internal carotid artery; f. = fold. © Edoardo Agosti, published with permission.

were exposed. A C-shaped durotomy was performed that was centered on the sylvian fissure, exposing the intradural structures. Wide exposure of the parasellar region and lateral wall of the cavernous sinus was afforded. The key surgical anatomy and steps of the 3-piece orbito-zygomatic craniotomy can be seen in Fig. 7.

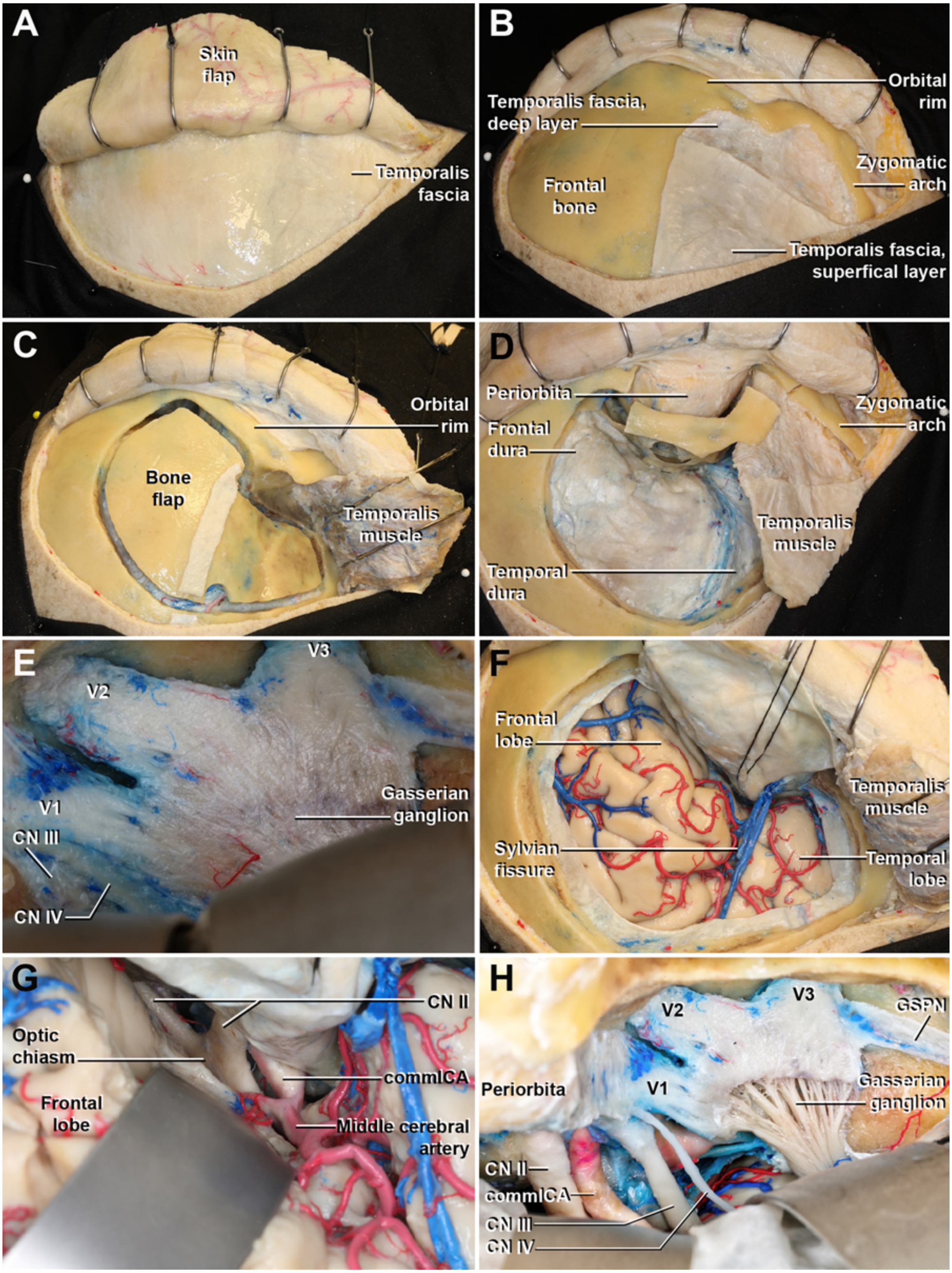

FIG. 7. Right-sided 3-piece orbito-zygomatic craniotomy. **A:** Curvilinear skin incision beginning just inferior to the root of the zygoma and extending to the midline hairline. **B:** Interfascial dissection. **C:** Standard pterional craniotomy. **D:** Osteotomies of the roof and lateral wall of the orbit and a separate osteotomy of the zygomatic arch. **E:** Epidural dissection and opening of Meckel's cave. **F:** Intradural exposure after a C-shaped durotomy centered over the sylvian fissure was performed. **G:** View of the carotid bifurcation and optic nerves. **H:** Transcavernous approach. commICA = communicating segment of internal carotid artery. © Edoardo Agosti, published with permission.

Discussion

Various approaches with many variations have been developed to address lesions within and around the orbit, each with its distinct advantages and limitations.

Of the approaches to and through the orbit, the transorbital approaches were the most recently described and utilized in the clinical setting. Several studies have described their efficacy in approaching lesions of the medial sphenoid wing, cavernous sinus, and petrous apex.[2,3,7–10,14,16] Several incisions have been described, including preseptal, eyelid, and lateral canthotomy or a combination of these.[4–6] The preseptal lower eyelid approach is suitable for procedures involving the lower or medial orbit. A superior eyelid incision is made directly on the eyelid, usually parallel to the eyelid crease, and medial to the supraorbital notch. Depending on the procedure, the incision may extend laterally. This approach provides direct access to the superior and lateral orbital walls and is often used in combination with other incisions for broader exposure. The lateral canthus is the outer corner of the eye where the upper and lower eyelids meet. Lateral canthotomy involves cutting the lateral canthal tendon, allowing for increased lateral mobility of the eyelid. This can be combined with other incisions for enhanced exposure, particularly in procedures requiring access to the lateral orbit.[6]

ETOAs have been associated with a low rate of ocular morbidity in the literature. Although the findings in the literature are favorable, one must consider that most series are published by a few centers that are highly specialized in transorbital surgery for cranial base lesions. For surgeons and centers aiming to incorporate transorbital approaches into their practices, experienced authors suggest starting with smaller extradural lesions with restricted anatomical extension before moving to more complex skull base pathology.[6] Multidisciplinary teams that include oculoplastic surgeons, otolaryngologists, and neurosurgeons are essential for successful execution of transorbital approaches.[4]

With several approaches to the orbit available, approach selection is crucial to successfully address cranio-orbital pathology. With regard to EEAs, these should be used when the lesion is medial to the ON in the anterior fossa, parasellar region, and orbit.[7,10,15] The main advantage of the EEAs is the obviation of brain retraction and, unlike any other approach described, the ability to visualize the medial and inferior ON from the OC proximally to the globe distally. To prevent enophthalmos, preservation of the inferomedial strut of the bony orbit is crucial. The main advantage of the supraorbital and fronto-orbital approaches is the wide exposure they provide of the parasellar region and anterior cranial fossa. For lesions extending into the middle cranial fossa and cavernous sinus, a frontotemporal craniotomy is usually required, as the supraorbital approach provides limited access to the skull base posteroinferior to the lesser wing of the sphenoid.[1] Orbit osteotomy and zygomatic osteotomy should be utilized when a superior trajectory in the parasellar region and middle fossa is required. The indications for ETOAs are still debated given the novelty of these approaches in the armamentarium of the skull base surgeon. The transorbital approaches bring a new perspective of the anatomy that is relatively unfamiliar to the neurosurgical community as compared to the transcranial approaches. Depending on surgeon comfort, these approaches can provide anatomical access to the anterior cranial fossa, middle fossa, cavernous sinus, and petrous apex.[4–6]

Conclusions

We have described the key surgical steps and exposure of the main cranio-orbital and orbitocranial approaches used to integrate different anatomical perspectives into a 360° comprehensive view and to provide exposure to and through the orbit. EEAs provide direct medial access to the orbit, offering the potential for bilateral exposure to the OCs. ETOAs can be employed for both orbital access and as a surgical corridor to reach regions around the orbit. Cranio-orbital approaches follow a lateral-to-medial and superior-to-inferior trajectory, gradually removing protective bony structures to provide proportional access to the orbit.

Acknowledgments

The present study was conducted with the support of the NeuroAnatomy Committee of the Italian Society of Neurosurgery (SINch). We extend our gratitude to the members for their invaluable contributions and expertise that greatly enhanced the quality of this research. We acknowledge Charles “Wes” Price, MS, CMI, for his contributions to editing and processing of our photogrammetry 3D models. This work was supported in part by the Joseph I. and Barbara Ashkins Endowed Professorship in Neurosurgery and the Charles B. and Ann L. Johnson Endowed Professorship in Neurosurgery.

References

1. Abou-Al-Shaar H, Krisht KM, Cohen MA, et al. Cranio-orbital and orbitocranial approaches to orbital and intracranial disease: eye-opening approaches for neurosurgeons. *Front Surg*. 2020;7:1.
2. Bander ED, Carnevale JA, Tosi U, Godfrey KJ, Schwartz TH. Lateral transorbital endoscope-assisted approach to the cavernous sinus. *Oper Neurosurg (Hagerstown)*. 2023;25(4):359-364.
3. Carnevale JA, Rosen KU, Chae JK, et al. The endoscopic lateral transorbital approach for the removal of select sphenoid wing and middle fossa meningiomas. Surgical technique and short-term outcomes. *Oper Neurosurg (Hagerstown)*. 2024;26(2):165-172.
4. Dallan I, Cristofani-Mencacci L, Fiacchini G, Caniglia M, Sellari-Franceschini S, Berrettini S. When multidisciplinary surgical trans-orbital approaches should be considered to reach the skull base. *Acta Otorhinolaryngol Ital*. 2021;41(Suppl 1):S59-S66.
5. Di Somma A, Andaluz N, Cavallo LM, et al. Endoscopic transorbital superior eyelid approach: anatomical study from a neurosurgical perspective. *J Neurosurg*. 2018;129(5):1203-1216.
6. Di Somma A, Kong DS, de Notaris M, et al. Endoscopic transorbital surgery levels of difficulty. *J Neurosurg*. 2022;137(4):1187-1190.
7. Jeon C, Hong SD, Woo KI, et al. Use of endoscopic transorbital and endonasal approaches for 360° circumferential access to orbital tumors. *J Neurosurg*. 2020;135(1):103-112.
8. Kong DS, Kim YH, Lee WJ, Kim YH, Hong CK. Indications and outcomes of endoscopic transorbital surgery for trigeminal schwannoma based on tumor classification: a multicenter study with 50 cases. *J Neurosurg*. 2022;138(6):1653-1661.

9. Kong DS, Shin HJ. Endoscopic transorbital surgery for trigeminal schwannoma: introduction of a novel approach: 2-dimensional operative video. *Oper Neurosurg (Hagerstown).* 2024;26(1):96-97.
10. Lee WJ, Hong SD, Woo KI, et al. Endoscopic endonasal and transorbital approaches to petrous apex lesions. *J Neurosurg*. 2021;136(2):431-440.
11. Locatelli D, Pozzi F, Turri-Zanoni M, et al. Transorbital endoscopic approaches to the skull base: current concepts and future perspectives. *J Neurosurg Sci*. 2016;60(4):514-525.
12. MacCarty CS. Surgical techniques for removal of intracranial meningiomas. *Clin Neurosurg*. 1959;7:100-111.
13. Marcellino CR, Peris-Celda M, Link MJ, Stokken JK. Endoscopic endonasal resection of orbital apex cavernous hemangioma: 2-dimensional operative video. *Oper Neurosurg (Hagerstown).* 2019;16(5):E144-E145.
14. Mathios D, Bobeff EJ, Longo D, et al. The lateral transorbital approach to the medial sphenoid wing, anterior clinoid, middle fossa, cavernous sinus, and Meckel's cave: target-based classification, approach-related complications, and intermediate-term ocular outcomes. *J Neurosurg*. 2024;140(3):677-687.
15. Salgado-Lopez L, Leonel LCPC, O'brien M, et al. Anatomical step-by-step dissection of complex skull base approaches for trainees: endoscopic endonasal approach to the orbit. *J Neurol Surg B Skull Base*. 2022;84(1):79-88.
16. Serioli S, Nizzola M, Plou P, et al. Surgical anatomy of the microscopic and endoscopic transorbital approach to the middle fossa and cavernous sinus: anatomo-radiological study with clinical applications. *Cancers (Basel).* 2023; 15(18):4435.
17. Tubbs RS, Loukas M, Shoja MM, Cohen-Gadol AA. Refined and simplified surgical landmarks for the MacCarty keyhole and orbitozygomatic craniotomy. *Neurosurgery*. 2010;66(6 Suppl Operative):230-233.
18. Leonel LCP, Carlstrom LP, Graffeo CS, et al. Foundations of advanced neuroanatomy: technical guidelines for specimen preparation, dissection, and 3D-photodocumentation in a surgical anatomy laboratory. *J Neurol Surg B Skull Base*. 2021; 82(Suppl 3):e248-e258.

Disclosures

The authors report no conflict of interest concerning the materials or methods used in this study or the findings specified in this paper.

Author Contributions

Conception and design: Peris Celda, Agosti, Alexander, Pinheiro Neto. Acquisition of data: Agosti, Alexander, Plou, De Bonis, Bauman, García-Lliberós, Piazza, Torregrossa. Analysis and interpretation of data: Agosti, Alexander. Drafting the article: Agosti, Alexander, Piazza. Critically revising the article: Peris Celda, Agosti, Alexander, Plou, Leonel, De Bonis, Bauman, Torregrossa, Pinheiro Neto. Reviewed submitted version of manuscript: Peris Celda, Agosti, Alexander, Plou, De Bonis, Bauman, Torregrossa, Pinheiro Neto. Approved the final version of the manuscript on behalf of all authors: Peris Celda. Administrative/technical/material support: Agosti, García-Lliberós, Torregrossa. Study supervision: Peris Celda, Agosti.

Supplemental Information

Videos

Video 1. https://vimeo.com/910903238.

Correspondence

Maria Peris Celda: Mayo Clinic, Rochester, MN. periscelda.maria@mayo.edu.